SEMARAK ILMU PUBLISHING

Journal of Advanced Research in Fluid Mechanics and Thermal Sciences

Journal homepage:
https://semarakilmu.com.my/journals/index.php/fluid_mechanics_thermal_sciences/index
ISSN: 2289-7879

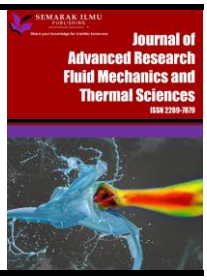

The Effective and Exergy Efficiency of Multi-Pass Solar Air Collector with Longitudinal Fins: Analysis and Optimization

Le Minh Nhut[1], Ha Nguyen Minh[2], Luan Nguyen Thanh[1,*]

[1] Faculty of Vehicle and Energy Engineering, Ho Chi Minh City University of Technology and Education (HCMUTE), Vietnam
[2] Faculty of Mechanical Engineering, University of Transport and Communications, Hanoi, Vietnam

ARTICLE INFO

Article history:
Received 15 August 2022
Received in revised form 16 December 2022
Accepted 27 December 2022
Available online 15 January 2023

Keywords:
Effective efficiency; exergy efficiency; multi-pass solar air collector; longitudinal fins; multi-objective optimization; the PSI method

ABSTRACT

The present work investigates the exergy and effective efficiency of the multi-pass solar air collector with longitudinal fins by analysis approach and multi-objective optimization. The effect of 0.01-0.02 kg/s air flow rate, 15-35 mm collector depth, 1-3 m collector length, and 24.21-30.67 mm fin pitch was considered. The optimization was analyzed by the Preference Selection Index (PSI) method, with three maximum criteria: thermal efficiency, effective efficiency, and exergy efficiency. Mathematical models were solved by EES software. Results indicated that the multi-pass (TPLF and DPLF) type was better than the SPWF type by three criteria. The highest exergy efficiency of the TPLF and DPLF types was 6.696% and 5.636%. The greatest effective efficiency of the TPLF and DPLF types was 69.09% and 66.17%. Furthermore, the optimization results indicated that the three efficiency criteria of the DPLF type were 58.38%, 58.22%, and 4.491% for the best case; the three efficiency criteria of the TPLF type were 60.97%, 60.85%, and 5.439% for the best case. The worst configuration was the model with a short collector length, large collector depth, and large fin pitch. The collector efficiency decreased with decreased fin pitch for the configuration with the large collector length, short collector depth, and high mass flow rate.

1. Introduction

In recent years, the rapid reduction of natural resources and climate change has spurred countries to adopt sustainable operating practices. Economic growth increases CO_2 emissions, so net zero emissions and sustainable development goals are set for countries [1,2]. Transitioning to a low-carbon fuel or renewable energy source in the future is essential to meeting sustainable development goals [3-5]. Solar energy is an available source with large reserves, so the potential for use is huge [6]. This energy source is an energy use strategy for many countries, including Vietnam. Many devices exploit this energy source, such as solar batteries, solar water collectors, solar air collectors, etc. The energy systems with the assistance of solar energy led to reduce costs and are environmentally beneficial [7]. Among devices using solar energy, the solar air collector (SAC) is used to heat the air

* *Corresponding author.*
E-mail address: luannt@hcmute.edu.vn

https://doi.org/10.37934/arfmts.102.2.4265

for drying or heating. It is a form of solar energy exploitation widely applied in life and production because of its simplicity in manufacturing and operation. However, the air convective heat transfer coefficient is low, so its improvement is essential. There are several solutions to this problem, such as adding a rib or fins on the absorber plate, adding the baffle inside the air channel, using a jet plate, or using a corrugated absorber plate. Wire rib, V-Rib, W-Rib, triangle rib, square rib, rectangular fin, semicircular fin, triangular fin, round pin fin, wavy fin, inclined baffle, jets plate, corrugated plate as the solutions have been investigated with promising results [8-28]. In addition, some solutions combined solar energy storage to enhance the performance and uptime of the units after sunset, or some evacuated tube solar air collectors or concentrated forms have significantly improved efficiency compared to the traditional form [29-32]. Furthermore, some studies looking at replacing metal absorber plates with other materials were also surveyed [33-35]. Several studies on heat loss reduction through the wall of collector have also been considered [36,37]. All solutions show improved collector efficiency.

In addition, some studies demonstrate that the collector with multi-pass airflow can enhance thermal efficiency (TEF) due to reducing heat loss at the top of SAC and increasing air temperature. Combined solutions have also been considered in many studies. The multi-pass SAC with longitudinal fins is one of those. Velmurugan and Kalaivanan [38] investigated the multi-pass SAC by the analytical approach. These authors found the highest TEF for triple-pass SAC and the better economy for the double-pass SAC. Naphon [39] and Fudholi *et al.,* [40] experimentally studied a double-pass SAC. They reported that the TEF increased with fin height and fin number. The TEF of double-pass SAC with a longitudinal fin can reach about 71.37% at m = 0.04kg/s and I = 600 W/m^2, which is a promising result. It is better than a single-pass SAC with other fin types. Garg *et al.,* [41] reported a 40-61% TEF for a single-pass SAC with fins. Sivakumar *et al.,* [42] evaluated a single-pass SAC with a round pin fin; they reported that the maximum TEF was 38%. Hosseini *et al.,* [43] reported the TEF was less than 60% for single-pass SAC with triangular fin. Manjunath *et al.,* [44] reported TEF of 65 % for a single-pass SAC with spherical fins at m=0.04kg/s and I=500W/m^2. Chabane *et al.*, [18] noted the highest TEF of 51.5% for single-pass SAC with semi-cylindrical fins.

Besides assessing the TEF, recent exergy efficiency (EXEF) and optimization analyses have been interested [23,45]. It evaluates more comprehensively and could determine the best configuration for the actual production. Hedayatizadeh *et al.,* [46] evaluated SAC with a V-corrugated absorber plate. They determined the optimal configuration with the greatest EXEF of 6.27%. Luan and Phu [47] analyzed the EXEF and optimization of multi-pass SAC with a flat absorber plate. They reported the highest EXEF of 4.7% for the best case of the triple-pass SAC. Farahani and Shadi [48] examined SAC with an impingement jet. They suggested an optimal model of SAC with the highest EXEF of 1.58%. The above studies indicated that exergy analysis and multi-objective optimization had been considered in many different SAC configurations.

The literature review showed that multi-pass SAC with longitudinal fins significantly improved heat transfer capacity due to increased heat exchange area, enhanced mixing of primary and secondary airflow, and reduced heat loss of the top collector. It is a promising solution with good results. The TEF is assessed based on useful thermal energy gain. The effective efficiency (EEF) is assessed based on useful thermal energy gain and fan energy consumed. The EXEF refers to irreversibility, demonstrating the ability to generate useful work in a thermal system. The TEF criterion is not enough to evaluate the performance of the SAC in practice. Therefore, the EEF and EXEF criteria need to be considered. It was not found in previous studies for that multi-pass SAC with longitudinal fins. Moreover, many factors affect collector efficiency, and choosing the optimal configuration for practice is significant in the goal of efficient energy use and sustainable development. The three efficiency type has different evaluation criteria. Therefore, choosing an

optimal design configuration that harmonizes according to these three criteria is necessary. Thus, the primary purpose of the present study was to examine the effects of the collector length, collector depth, fin pitch, and air flow rate on the EEF and EXEF of multi-pass SAC with longitudinal fins. Furthermore, multi-objective optimization according to the three maximum criteria of the TEF, EEF, and EXEF was considered in this study to select the best configuration according to the goal of harmonization in design. Results can be referenced for the design directly related to this type of collector.

2. Methodology

2.1 Geometry Model and Energy Balance

Figure 1 displays the geometry of SAC in this study, including the double-pass with longitudinal fins (DPLF) type and triple-pass with longitudinal fins (TPLF) type [38]. The two models have double glass.

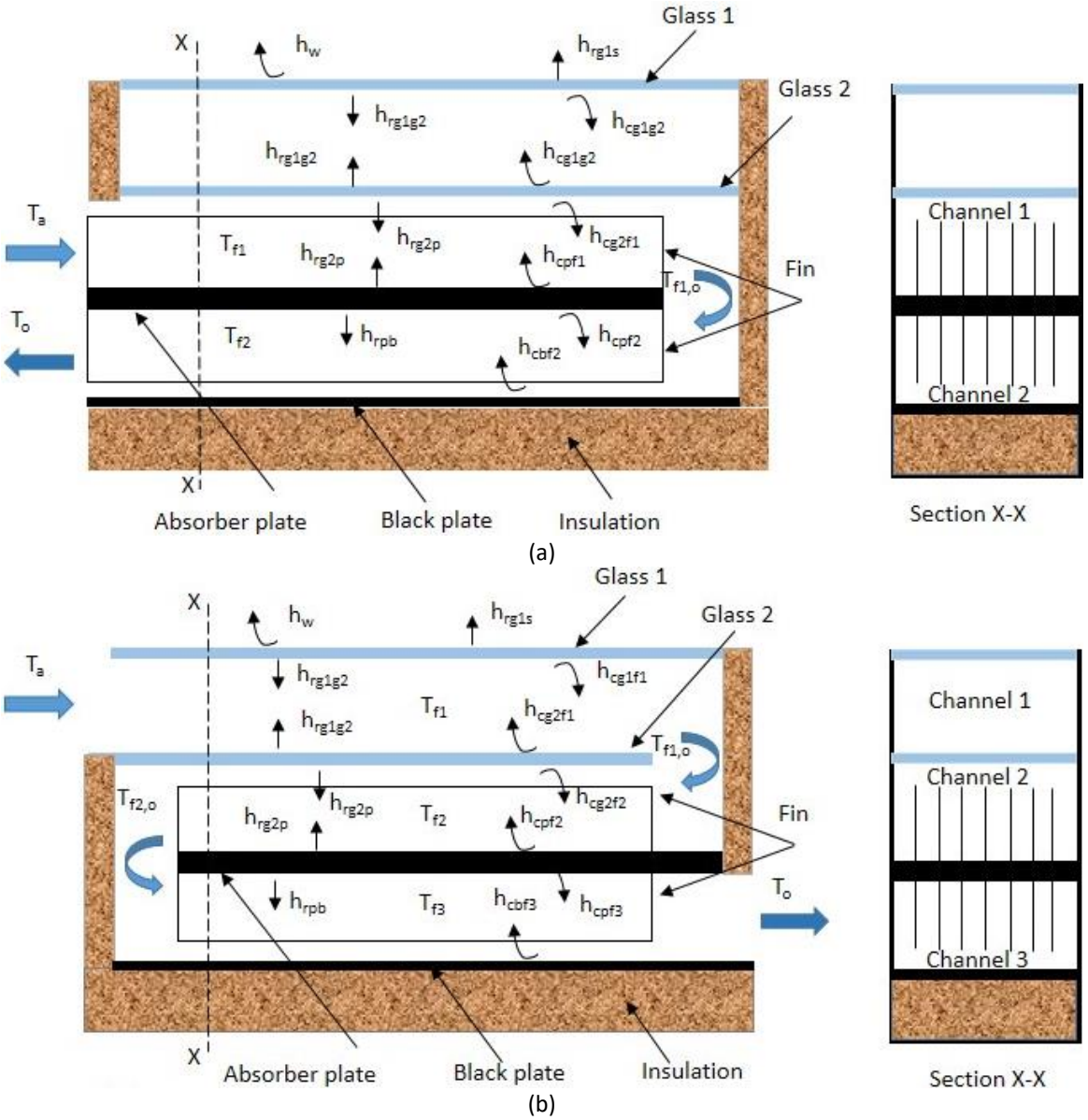

Fig. 1. Geometry of multi-pass type with longitudinal fins (a) double-pass type (b) triple-pass type [38]

The assumptions made in this study include [47,49]

i. Flow is steady and one-dimensional.
ii. Air is an ideal gas, incompressible and ignore potential and kinetic energy effects.
iii. The temperatures of plates are homogeneous. Thermophysical properties of plates are constants and ignore the heat loss on both wall sides.

The energy balance for the DPLF type is represented by the following, see Figure 1(a)

Glass 1

$$\alpha_{g1}.I = h_w(T_{g1}-T_a) + h_{rg1s}(T_{g1}-T_s) + h_{cg1g2}(T_{g1}-T_{g2}) + h_{rg1g2}(T_{g1}-T_{g2}) \quad (1)$$

Glass 2

$$\alpha_{g2}.\tau_{g1}.I = h_{cg1g2}(T_{g2}-T_{g1}) + h_{rg1g2}(T_{g2}-T_{g1}) + h_{cg2f1}(T_{g2}-T_{f1}) + h_{rg2p}(T_{g2}-T_p) \quad (2)$$

Fluid flow 1

$$Q_{f1} = A_c h_{cg2f1}(T_{g2}-T_{f1}) + A_c h_{cpf1}(T_p-T_{f1})\theta \quad (3)$$

where θ dimensionless quantity related to fins, which is determined as [38]:

$$\theta = 1 + (2NW_f L_f/A_c).tanh[2W_f h_{cpf}/(k_p t_f)]/[2W_f h_{cpf}/(k_p t_f)] \quad (4)$$

Fluid flow 2

$$Q_{f2} = A_c h_{cbf2}(T_b-T_{f2}) + A_c h_{cpf2}(T_p-T_{f2})\theta \quad (5)$$

Absorber plate

$$\alpha_p.\tau_{g1}.\tau_{g2}.I = h_{cpf1}(T_p-T_{f1})\theta + h_{cpf2}(T_p-T_{f2})\theta + h_{rg2p}(T_p-T_{g2}) + h_{rpb}(T_p-T_b) \quad (6)$$

Black plate

$$h_{rpb}(T_p-T_b) = h_{cbf2}(T_b-T_{f2}) + h_i(T_b-T_a) \quad (7)$$

The energy balance equations for the triple -pass type with fins (TPLF) type (see Figure 1(b)) can be seen below. Furthermore, the single-pass without fins (SPWF) type was used to compare the performance with the multi-pass type for a visual look.

For TPLF, see Figure 1(b)

Glass 1

$$\alpha_{g1}.I = h_w(T_{g1}-T_a) + h_{rg1s}(T_{g1}-T_s) + h_{cg1f1}(T_{g1}-T_{f1}) + h_{rg1g2}(T_{g1}-T_{g2})$$

Fluid flow 1

$$Q_{f1} = A_c h_{cg1f1}(T_{g1} - T_{f1}) + A_c h_{cg2f1}(T_{g2} - T_{f1})$$

Glass 2: $\alpha_{g2}.\tau_{g1}.I = h_{cg2f1}(T_{g2} - T_{f1}) + h_{cg2f2}(T_{g2} - T_{f2}) + h_{rg1g2}(T_{g2} - T_{g1}) + h_{rg2p}(T_{g2} - T_p)$

Fluid flow 2

$$Q_{f2} = A_c h_{cg2f2}(T_{g2} - T_{f2}) + A_c h_{cpf2}(T_p - T_{f2})\theta$$

Absorber plate

$$\alpha_p.\tau_{g1}.\tau_{g2}.I = h_{cpf2}(T_p - T_{f2})\theta + h_{cpf3}(T_p - T_{f3})\theta + h_{rg2p}(T_p - T_{g2}) + h_{rpb}(T_p - T_b)$$

Fluid flow 3

$$Q_{f3} = A_c h_{cbf3}(T_b - T_{f3}) + A_c h_{cpf3}(T_p - T_{f3})\theta$$

Black plate

$$h_{rpb}(T_p - T_b) = h_{cbf3}(T_b - T_{f3}) + h_i(T_b - T_a)$$

The energy balance equations and geometry can be viewed in Figure 2 below.

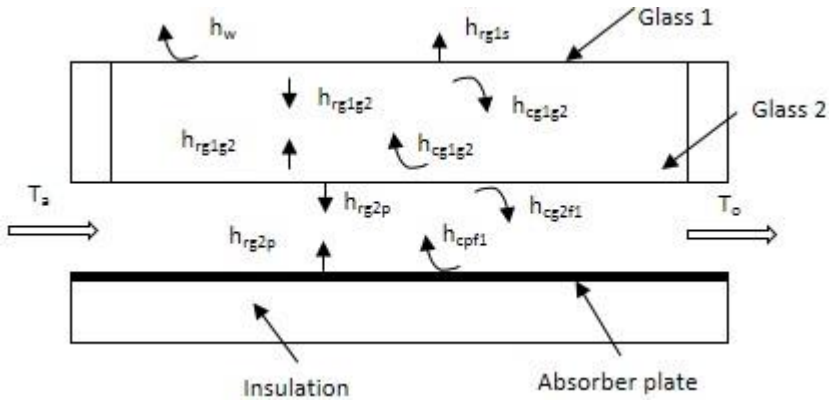

Fig. 2. The single -pass type without fins (SPWF)

Glass 1

$$\alpha_{g1}.I = h_w(T_{g1} - T_a) + h_{rg1s}(T_{g1} - T_s) + h_{cg1g2}(T_{g1} - T_{g2}) + h_{rg1g2}(T_{g1} - T_{g2})$$

Glass 2

$$\alpha_{g2}.\tau_{g1}.I = h_{cg1g2}(T_{g2} - T_{g1}) + h_{cg2f1}(T_{g2} - T_{f1}) + h_{rg1g2}(T_{g2} - T_{g1}) + h_{rg2p}(T_{g2} - T_p)$$

Fluid flow

$$Q_{f1} = A_c h_{cg2f1}(T_{g2} - T_{f1}) + A_c h_{cpf1}(T_p - T_{f1})$$

Absorber plate

$$\alpha_p.\tau_{g1}.\tau_{g2}.I = h_{cpf1}(T_p - T_{f1}) + h_{rg2p}(T_p - T_{g2}) + h_i(T_p - T_a)$$

The heat transfer coefficient (HTC) is calculated by the formulas

The convective HTC between glass 1 with the wind is calculated by the formula [47]

$$h_w = 5.7 + 3.8V_w \quad (8)$$

The radiation HTC from glass 1 to the sky is calculated as follows [50,51]

$$h_{rg1s} = \sigma.\varepsilon_g(T_{g1}^2 + T_s^2)(T_{g1} + T_s) \quad (9)$$

where $T_s = T_a - 6$ is the sky temperature *for* clear-sky condition.

The conductive HTC through the insulation is calculated by the formula [51]

$$h_i = k_i/t_i \quad (10)$$

The natural convective HTC between two glasses is calculated as follows [52]

$$h_{cg1g2} = 1.25(T_{g2} - T_{g1})^{0.25} \quad (11)$$

The convective HTC between the air with surfaces can be determined [38]

$$h_{cgf} = h_{cpf} = h_{cbf} = Nu.k/D_h \quad (12)$$

where D_h and Nu are the hydraulic diameter and the Nusselt number, respectively.

The hydraulic diameter of can be determined

$$D_h = \frac{4HB}{2(H+B)} \quad (13)$$

The Nusselt number is calculated as follows [38,50]

$Nu_s = 0.023Re^{0.8}Pr^{0.4}$, for smooth channel (14)

$Nu_f = 0.018Re^{0.8}Pr^{0.4}$, for channel with longitudinal fins (15)

The radiation HTC between surfaces is calculated as follows [50]

$$h_{rg1g2} = \sigma(T_{g1}^2 + T_{g2}^2)(T_{g1}+T_{g2})/(1/\varepsilon_{g1} + 1/\varepsilon_{g2} - 1) \quad (16)$$

$$h_{rg2p} = \sigma(T_{g2}^2 + T_p^2)(T_{g2}+T_p)/(1/\varepsilon_{g2} + 1/\varepsilon_p - 1) \quad (17)$$

$$h_{rpb} = \sigma\left(T_b^2 + T_p^2\right)\left(T_b + T_p\right)/\left(1/\varepsilon_b + 1/\varepsilon_p - 1\right) \quad (18)$$

2.2 Evaluation Criteria

There are three essential criteria to evaluate SAC efficiency: the TEF, EEF, and EXEF. The criterias are determined as follows

The useful heat received by the air can be determined [38,47]

$$Q_u = m.c_p.(T_o - T_a) \quad (19)$$

The TEF is calculated by the formula [38,47]

$$\eta_I = \frac{Q_u}{IA_c} \quad (20)$$

The energy consumption for fans is determined [38,47]

$$P_m = m.\Delta P/\rho \quad (21)$$

The pressure loss through the air channel can be determined [38,47]

$$\Delta P = \Delta P_s + \Delta P_{bend} \quad (22)$$

where ΔP_s and ΔP_{bend} are pressure drop along the channel and 180° return bend, respectively.

The pressure drop along the channel is calculated by the formula [38,47]

$$\Delta P_s = 2\rho f L V^2/D_h \quad (23)$$

where $f = 0.085\ Re^{-0.25}$ is friction factor for smooth channel; $f = 0.079 Re^{-0.25}$ is friction factor for channel with longitudinal fins.

The pressure drop for return bend is determined [38,47]

$$\Delta P_s = K_{bend}\rho V^2/2 \quad (24)$$

where K_{bend} is a loss factor for 180° return bend, $K_{bend} = 2.2$ [38,47].

The effective efficiency is calculated as follows [47,51]

$$\eta_{eff} = (Q - P_m/c_i)/(I.A) \quad (25)$$

where c_i is the conversion factor of fans power, $c_i = 0.2$ [53].

The energy of SAC received from the sun can be determined [49,54,55]

$$Q_s = \left(\alpha_p \tau_p\right).I.A_c \tag{26}$$

The supplied exergy to the SAC is estimated by the following [49,54,55]

$$Ex_{in} = (1 - T_a/T_{sun})Q_s \tag{27}$$

where T_{sun} is the sun temperature, $T_{sun} = 4350\ K$ [53].

The exergy of the inlet and outlet fluid is determined [49,54,55]

$$Ex_{i,air} = m(h_i - h_e) + m.T_e(s_i - s_e) \tag{28}$$

$$Ex_{o,air} = m(h_o - h_e) + m.T_e(s_o - s_e) \tag{29}$$

where h_e and s_e are specific enthalpy and specific entropy at ambient temperature, respectively.

The exergy equilibrium equation for a stable system [49]

$$Ex_{des} = Ex_{in} + Ex_{i,air} - Ex_{o,air} = \left(1 - \frac{T_a}{T_{sun}}\right) Q_s - m(h_o - h_i) - m.T_e(s_o - s_i) \tag{30}$$

The variation enthalpy and entropy of fluid is calculated as follows [49,54,55]

$$h_o - h_i = c_p(T_o - T_i) \tag{31}$$

$$s_o - s_i = c_p ln(T_o/T_a) - Rln[P_o/(P_o + \Delta P)] \tag{32}$$

From Eq. (31) and Eq. (32), the Eq. (30) can be rewritten

$$Ex_{des} = E_{in} - Q_u + mc_pT_a ln(T_o/T_a) - mRT_a ln[P_o/(P_o + \Delta P)] \tag{33}$$

The exergy efficiency is expressed as [54,55]

$$\eta_{II} = 1 - Ex_{des}/Ex_{in} \tag{34}$$

2.3 Multi-Objective Optimization Method

Using the optimization method is necessary to determine the best configuration in design. The preference selection index (PSI) method was chosen in many multi-objective optimization methods because its approach was clear and straightforward, and there was no need to select weights. [47,56,57]. This method has been widely applied in many fields in recent years [47,58]. This study selected three objective functions to determine the optimal configuration for multi-pass type with longitudinal fins: the maximum for the TEF, EEF, and EXEF. The calculation steps of this method can be carried out as follows [47,57,59]

Step 1: Normalization of criteria, for benefit criteria (higher is better)

$$b_{i,\eta_I} = \frac{\eta_I^i}{\eta_I^{max}}$$
$$b_{i,\eta_{eff}} = \frac{\eta_{eff}^i}{\eta_{eff}^{max}} \quad (35)$$
$$b_{i,\eta_{II}} = \frac{\eta_{II}^i}{\eta_{II}^{max}}$$

Step 2: Calculate the mean of the normalized criteria

$$M_{\eta_I} = \frac{1}{n}.\sum_{i=1}^{n} b_{i,\eta_I}$$
$$M_{\eta_{eff}} = \frac{1}{n}.\sum_{i=1}^{n} b_{i,\eta_{eff}} \quad (36)$$
$$M_{\eta_{II}} = \frac{1}{n}.\sum_{i=1}^{n} b_{i,\eta_{II}}$$

Step 3: Calculate preference variation value

$$\chi_{\eta_I} = \sum_{i=1}^{n}\left(b_{i,\eta_I} - M_{\eta_I}\right)$$
$$\chi_{\eta_{eff}} = \sum_{i=1}^{n}\left(b_{i,\eta_{eff}} - M_{\eta_{eff}}\right) \quad (37)$$
$$\chi_{\eta_{II}} = \sum_{i=1}^{n}\left(b_{i,\eta_{II}} - M_{\eta_{II}}\right)$$

Step 4: Calculate deviation of preference variation value

$$d_{\eta_I} = 1 - \frac{\chi_{\eta_I}}{n-1}$$
$$d_{\eta_{eff}} = 1 - \frac{\chi_{\eta_{eff}}}{n-1} \quad (38)$$
$$d_{\eta_{II}} = 1 - \frac{\chi_{\eta_{II}}}{n-1}$$

Step 5: Calculate overall preference value

$$\varepsilon_{\eta_I} = d_{\eta_I}/(d_{\eta_I} + d_{\eta_{eff}} + d_{\eta_{II}})$$
$$\varepsilon_{\eta_{eff}} = d_{\eta_{eff}}/(d_{\eta_I} + d_{\eta_{eff}} + d_{\eta_{II}}) \quad (39)$$
$$\varepsilon_{\eta_{II}} = d_{\eta_{II}}/(d_{\eta_I} + d_{\eta_{eff}} + d_{\eta_{II}})$$

Step 6: Calculate the PSI value

$$\theta_{PSI} = b_{i,\eta_I}\varepsilon_{\eta_I} + b_{i,\eta_{eff}}\varepsilon_{\eta_{eff}} + b_{i,\eta_{II}}\varepsilon_{\eta_{II}} \quad (40)$$

Figure 3 presents the algorithm diagrams for this study. Figure 3(a) is the algorithm diagram to survey the effects of parameters on the TEF and EXEF. Figure 3(b) is the algorithm diagram for the multi-objective optimization case. The systems of equations and calculations are solved by the Engineering Equation Solver (EES) software; this software was developed by Klein and Alvarado [60]. It is very convenient for solving systems of equations, with enough equations and variables, and the software will find the result quickly.

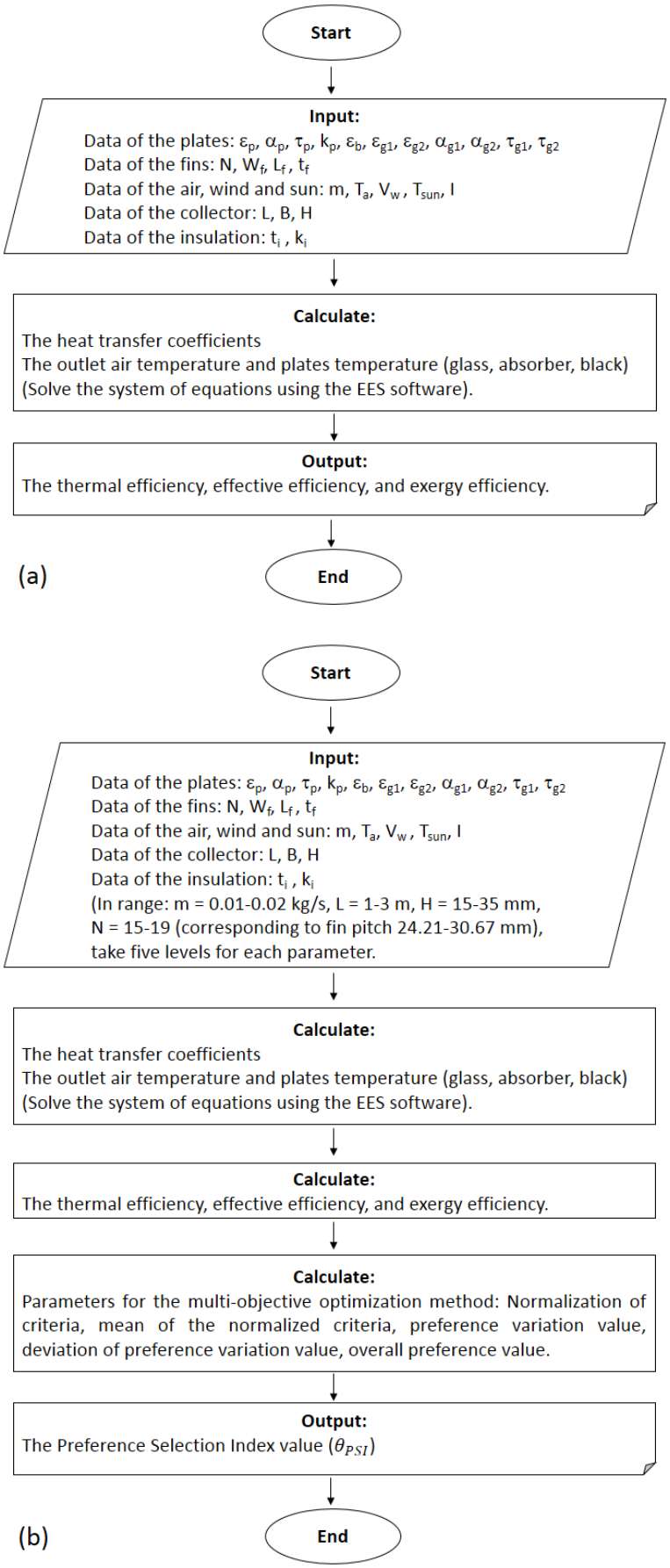

Fig. 3. The algorithm organigram (a) for influence survey (b) for multi-objective optimization

3. Validation of Analysis Results

In this part, to verify the accuracy of the calculations, validation has been performed with the input data as follows [38]: I = 1000 W/m^2, t_i = 50 mm, $\varepsilon_p = \varepsilon_b = 0.94$, $\varepsilon_{g1} = \varepsilon_{g2} = 0.9$, $\alpha_{g1} = \alpha_{g2} = 0.06$, $\alpha_p = 0.95$, $\tau_{g1} = \tau_{g2} = 0.84$, L = 2000 mm, B = 460 mm, H = W_f = 25 mm, L_f = L-20 mm, V_w = 1.5 m/s, t_f = 0.95 mm, N = 17, k_p = 50.2 W/m.K, T_a = 306 K, k_i = 0.025 W/m.K. The system of equations was solved by the EES software.

Figure 4 indicates the validation result, which is in good agreement with the analytical approach result by Velmurugan and Kalaivanan [38]. Further, the verification with the experimental result was also performed to assess the reliability of the mathematical model: the single-pass model was compared with the data of Yeh and Lin [61]. The double-pass model was compared with the data of Velmurugan and Kalaivanan [62]. The result shows that the average error is about 5.02% and 2.14^{o}C between the present study and the experiment results, respectively (see Figure 5). Therefore, the data in the results and discussion sections can be trusted.

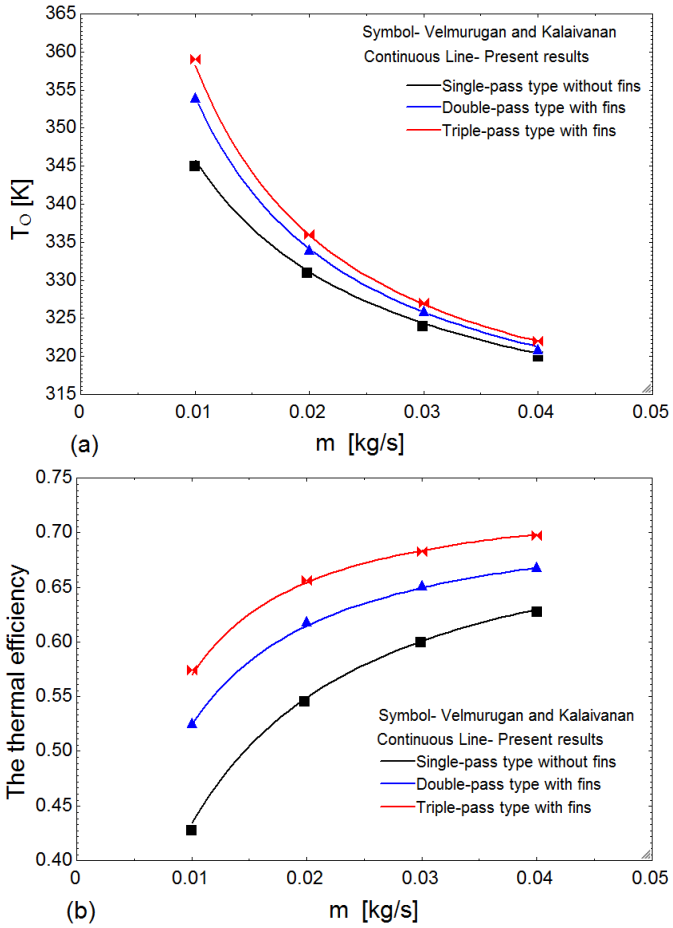

Fig. 4. Validation with previous publication (a) outlet temperature (b) thermal efficiency

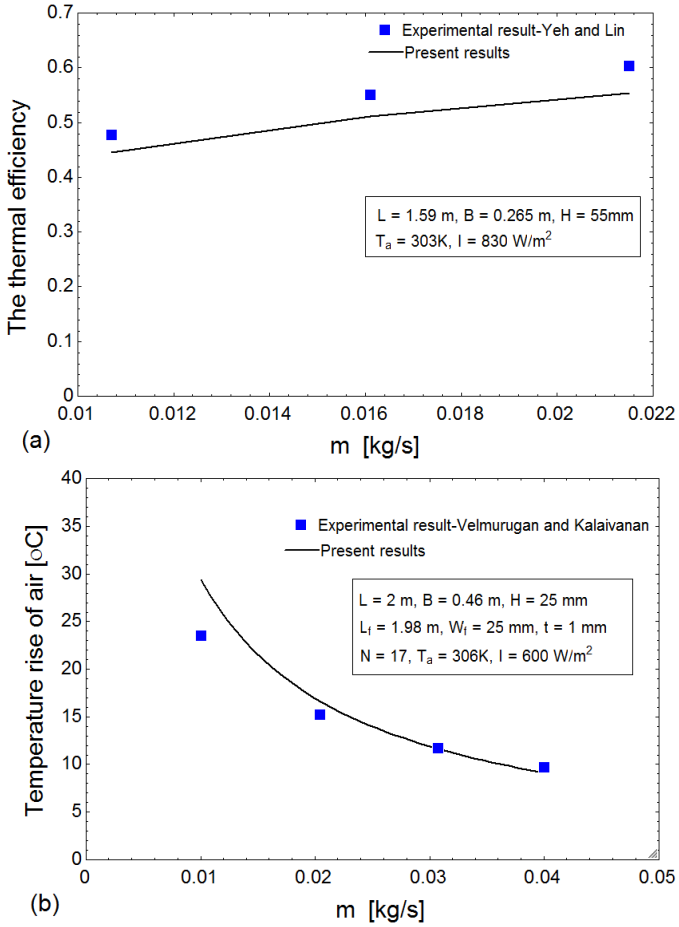

Fig. 5. Validation with previous experiment (a) Validation with Yeh and Lin [61] (b) Validation with Velmurugan and Kalaivanan [62]

4. Results and Discussion

The influence of operating and geometrical parameters on the EEF and EXEF and multi-objective optimization is discussed in this section. Figure 6 exhibits the impact of air flow rate on the EEF and EXEF in the case of fixing parameters as in section 3. The EEF increases with increasing air flow. The increased air flow rate increases the HTC, enhancing the heat received from the plates. The useful heat received increases, and the pressure drop also increases. However, the increase in the EEF proves that the pressure drop penalty is negligible. The multi-pass SAC with longitudinal fin has better efficiency than the SPWF, demonstrating that the heat loss at the top of the SAC decreases, and air temperature increases as movement over multiple passes. The EEF of multi-pass SAC approaches the EEF of the SPWF as air flow increases. It indicates that the pressure loss penalty is significant at a high flow rate. The highest EEF was 68.99% for the TPLF type and 66.3% for the DPLF type at m = 0.04 kg/s. The path length of multi-pass SAC is 2 and 3 times higher than the SPWF; the EEF difference is about 0.3-0.4% at a high flow rate.

The EXEF increases with the number of passes, highest at a low air flow rate. The EXEF tends to decrease with an increasing flow rate. A high flow rate leads to increased pressure loss, reduced air temperature, and reduced absorption plate temperature, which leads to increased exergy loss by fluid friction and heat transfer. The EXEF difference between multi-pass SAC and SPWF type is insignificant at a high flow rate. The EXEF of TPLF and DPLF types is about 5.888% and 5.024% at m = 0.01 kg/s, which is 2 and 3 times higher than the SPWF. Results show the opposite trend of the EEF and EXEF under the influence of air flow rate. The airflow rate from 0.01kg/s to 0.02 kg/s offers a good signal for both the EEF and EXEF.

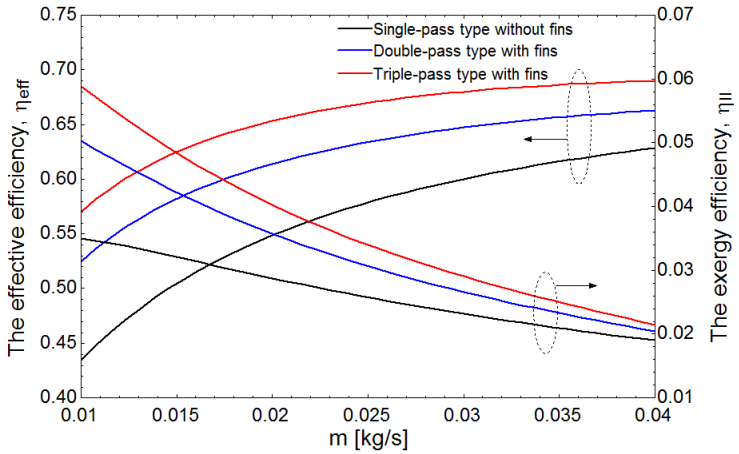

Fig. 6. Influence of air flow rate on the EEF, and EXEF

Figure 7 points to the influence of collector depth on outlet temperature, the EEF, and the EXEF at m= 0.02kg/s and fixed data as section 3. The outlet air temperature decrease with increasing collector depth. It can be explained by the fact that the air velocity decreased with increasing collector depth, leading to a decrease in heat exchange between the air and the surfaces, see Figure 7(a). The output temperature of the SPWF type is dropped more sharply than multi-pass SAC with fin. It shows that the using fin has significantly improved airflow mixing and enhanced heat exchange. The EEF of the TPLF type increases as H < 19.1 mm and decrease as H > 19.1 mm. Meanwhile, the DPLF and SPWF types tend to decrease as collector depth increases. It proves that increasing the number of passes and using fins can compensate for the impacts of collector depth.

The EXEF of the DPLF type increases as H < 16 mm and tends to decrease as H > 16 mm. The TPLF type increases the EXEF as H < 20.1 mm and decreases the EXEF as H > 20.1 mm, see Figure 7(b). It shows that the EXEF of multi-pass SAC with the fin is better at small collector depths. Increasing collector depth leads to a decrease in the EXEF due to increased exergy loss by heat transfer. The maximum EXEF of TPLF and DPLF types was 4.0386 % and 3.617 % at depth H = 20.1 mm and H = 16 mm, respectively. Increasing the collector depth is closely related to the air flow rate, influencing the trend of the EEF and EXEF. Therefore, the collector depth is a factor that needs to be considered in the design.

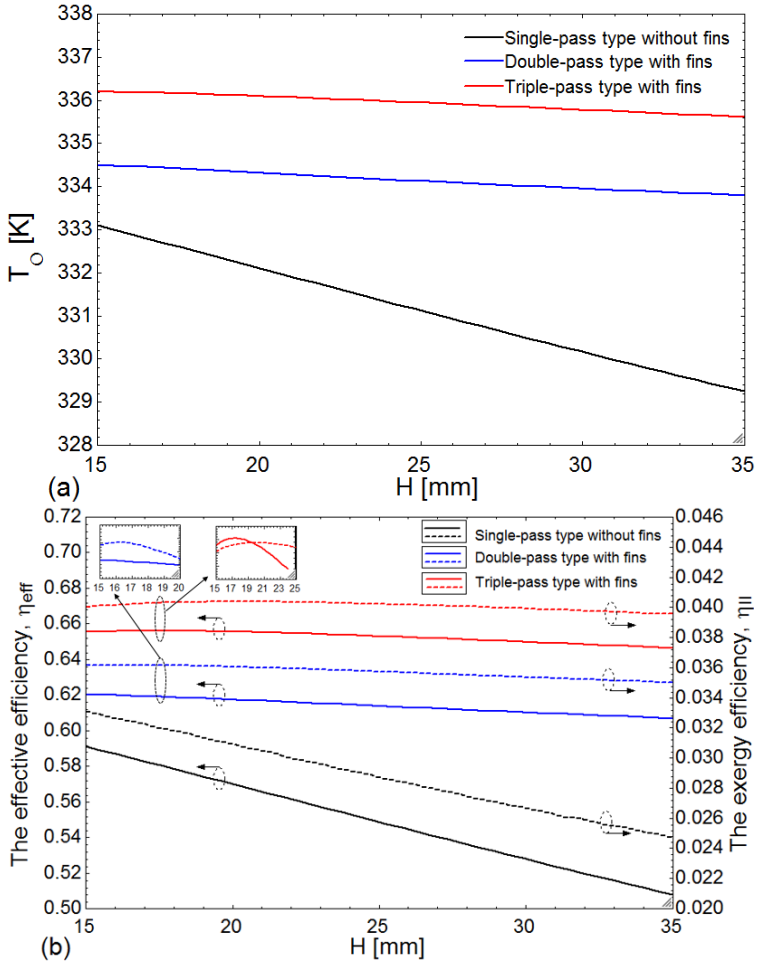

Fig. 7. Influence of collector depth (a) outlet temperature (b) the EEF and EXEF

Figure 8 demonstrates the influence of collector length on the outlet temperature, EEF, and EXEF at m = 0.01 kg/s and fixed data as in section 3. The outlet air temperature increases with the collector length because of an increase in the absorption area; see Figure 8(a). The outlet air temperature is highest for the TPLF type and lowest for the SPWF type. Increasing passes significantly increases the outlet air temperature. The EEF decreases with increasing collector length, which shows that the impact of pressure loss is significant; increasing the heat transfer does not compensate for energy loss due to increased pressure loss. The EXEF increases with collector length. It demonstrates that increasing the collector length decreases exergy loss by heat transfer, which can compensate for exergy loss by fluid friction. The highest EXEF is 6.676% for the TPLF type and 5.6% for the DPLF type at L = 3 m. The EEF and EXEF tend to be opposite with increasing collector length (see Figure 8(b)), so it is a parameter to consider in design.

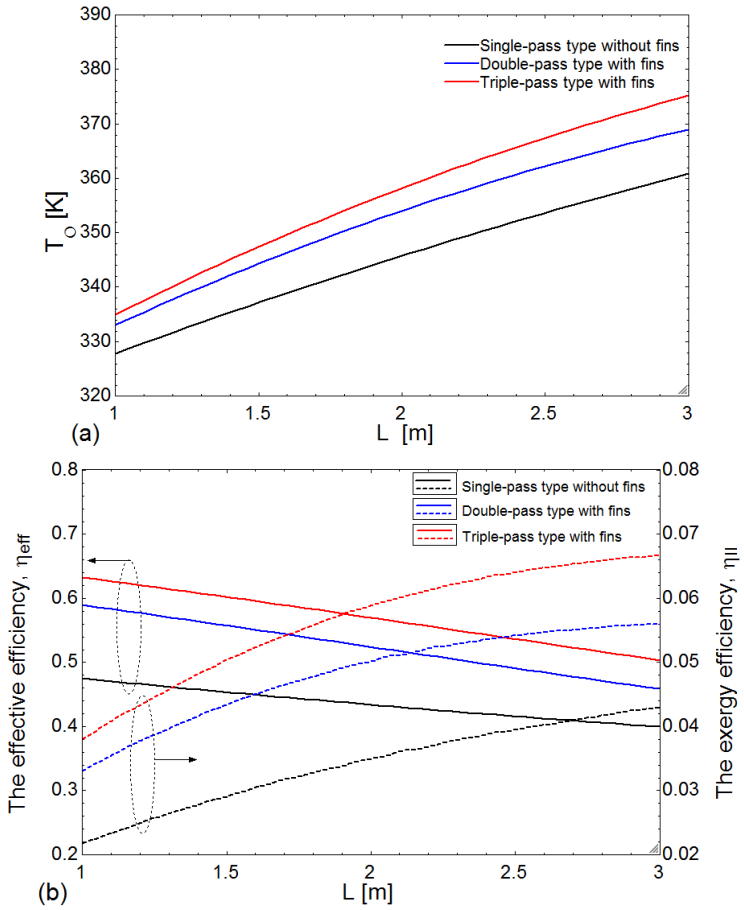

Fig. 8. Influence of collector length (a) outlet temperature (b) the EEF and EXEF

Figure 9 indicates the influence of fin pitch on the outlet air temperature, EEF, and EXEF at m = 0.01 kg/s and fixed data as in section 3. Increasing the fin pitch leads to a decrease in the number of fins, so the outlet temperature decreases due to a decrease in the heat exchange area and the ability to mix airflow; see Figure 9(a). The heat transfer capacity and pressure loss decrease with increased fin pitch. The reduction in pressure loss does not compensate for the reduction in useful heat received; exergy loss by heat transfer is significant, so the EEF and EXEF tend to decrease; see Figure 9(b). The efficiency and cost have tended to contrast with increasing fin pitch, so it is a parameter to consider in design.

From the analysis, the influence of the collector length, collector depth, fin pitch, and air flow rate have a contradictory influence on the EEF and EXEF. Therefore, choosing the optimal configuration for the design is necessary. The TEF, EEF, and EXEF are optimization targets, with the criteria: higher is better.

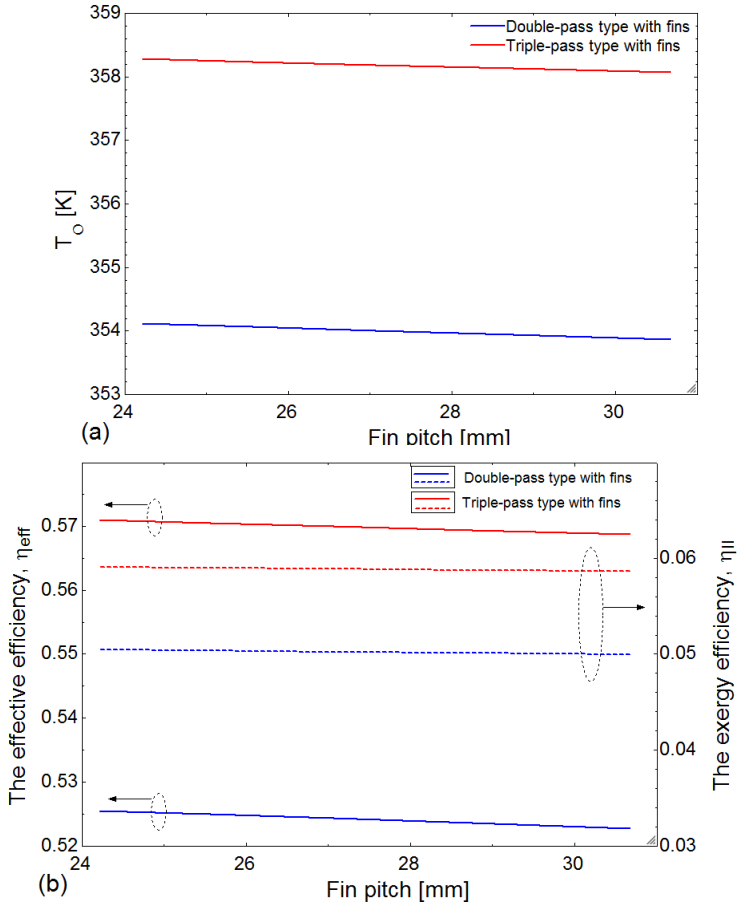

Fig. 9. Influence of fin pitch (a) outlet temperature (b) the EEF and EXEF

There are four parameters used for analysis to select the best configuration for multi-pass SAC with longitudinal fins, including collector length (1–3 m), collector depth (15–35 mm), fin pitch (24.21 mm, 25.56 mm, 27.06 mm, 28.75 mm, 30.67 mm), air mass flow rate (0.01–0.02 kg/s), take five levels for each parameter. Therefore, there are 625 cases to choose the best configurations for each SAC. Figure 10 shows the preference selection index value for 625 cases of each SAC. According to the results, the DPLF type has three best cases (451, 452, 326) and three worst cases (21, 521, 396), see Figure 10(a); the TPLF type has three best cases (179, 180, 481) and three worst cases (521, 522, 523), see Figure 10(b). The good configuration of the DPLF type with parameter L = 2.5 m, H = 15 mm, F_p = 28.75–30.67 mm, m = 0.15 – 0.175 kg/s. The good configuration of the TPLF type with parameter L = 2 m, H = 15 mm, F_p = 24.21–25.56 mm, m= 0.0125kg/s. These are configurations that can be referenced for design. These configurations are consistent with the previous analysis. The detail of the cases, parameters configuration, and rank are shown in Table 1.

According to the set goal, the best case for the DPLF type is case 451 with configuration (m = 0.0175 kg/s, H = 15 mm, L = 2.5 m, F_p = 30.67 mm), with the TEF, EEF, and EXEF are 58.38%, 58.22%, and 4.491%, respectively. The TEF, EEF, and EXEF are approximately 60.97%, 60.85%, and 5.439% for the best case of the TPLF type with configuration (m = 0.0125 kg/s, H = 15 mm, L = 2 m, F_p = 25.56 mm), respectively. Case 21 is worst for the DPLF type with configuration (m = 0.01 kg/s, H = 35 mm, L = 1 m, F_p = 30.67 mm), and case 521 is worst for the TPLF type with configuration (m = 0.02 kg/s, H = 35 mm, L = 1 m, F_p = 30.67 mm). The main characteristics of these configurations are short collector length, large collector depth, and large fin pitch, which are entirely consistent with the heat transfer theory.

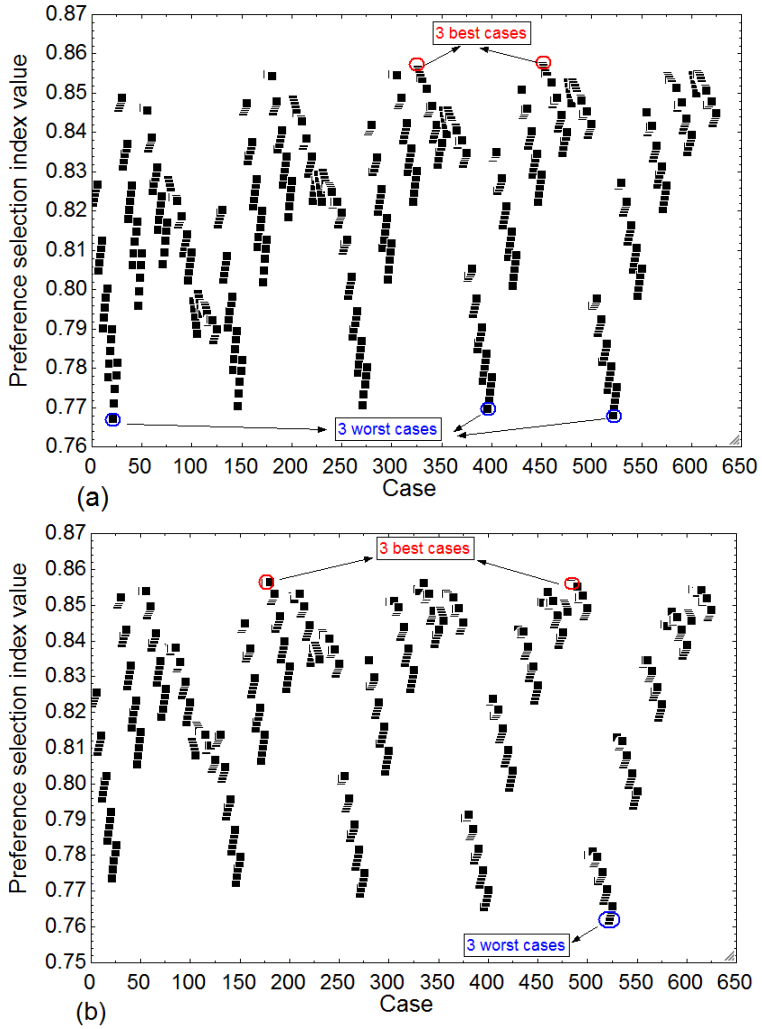

Fig. 10. Preference selection index value for 625 cases (a) the DPLF type (b) TPLF type

Table 1
Ranking of three best cases (1 to 3) and three worst cases (623 to 625), preference selection index value, configuration

Model	Case	Rank	θ_{PSI}	Parameter of solar air heater				Thermal efficiency, η_I	Effective efficiency, η_{eff}	Exergy efficiency, η_{II}
				Mass flow rate, m (kg/s)	Configuration					
					H(mm)	L(m)	F_p(mm)			
DPLF	451	1	0.8520	0.0175	15	2.5	30.67	0.5838	0.5822	0.04491
	452	2	0.8514	0.0175	15	2.5	28.75	0.5836	0.5819	0.04486
	326	3	0.8509	0.015	15	2.5	30.67	0.5626	0.5615	0.04838
	21	625	0.7621	0.01	35	1	30.67	0.5726	0.5725	0.03126
	521	624	0.7631	0.02	35	1	30.67	0.6392	0.6388	0.01984
	396	623	0.7647	0.0175	35	1	30.67	0.6288	0.6285	0.02191
TPLF	179	1	0.8564	0.0125	15	2	25.56	0.6097	0.6085	0.05439
	180	2	0.8564	0.0125	15	2	24.21	0.6097	0.6085	0.05439
	481	3	0.8563	0.0175	20	3	30.67	0.6004	0.5991	0.05623
	521	625	0.7618	0.02	35	1	30.67	0.6748	0.674	0.02199
	522	624	0.7629	0.02	35	1	28.75	0.6756	0.6749	0.02205
	523	623	0.7639	0.02	35	1	27.06	0.6764	0.6757	0.02210

In 625 surveyed cases, the highest EXEF of the DPLF and TPLF types is 5.636% and 6.698% for the configuration with parameters m = 0.01 kg/s, H = 20 mm, L = 3 m, and F_p = 30.67 mm. The highest EEF of the DPLF and TPLF types is 66.17% and 69.09% at m = 0.02 kg/s, H = 15 mm, L = 1 m, and F_p = 24.21 mm. Table 2 compares the highest EXEF between the present model and previous studies. The results show that the present model has certain advantages regarding the EXEF.

Table 2
Comparison of the highest EXEF of the present model and previous studies

Collector type	Reference	Comment
Double-pass, double glass and v-corrugated plate	Hedayatizadeh *et al.,* [46]	The highest EXEF was 6.27%
Double-pass, double glass, fins and phase change material	Assadeg *et al.,* [63]	The highest EXEF was 2.5–4.2%
Single-pass, 11 roughness shapes type	Phu and Luan [51]	The EXEF was less than 2% for eleven rib type
Single-pass, double glass, using rectangular fins or triangular fins	Bahrehmand *et al.,* [64]	The EXEF less than 2%
Double-pass with porous material	Abo-Elfadl *et al.,* [65]	The highest EXEF was 3.6 %
Double-pass with V-shaped finned Jet pate	Abo-Elfadl *et al.,* [66]	The highest EXEF was 2.5 %
Double-Pass with V rib-roughened	Matheswaran *et al.,* [53]	The highest EXEF was 4.36 %
Double-pass, double glass and longitudinal fins	Singh *et al.,* [67]	The EXEF was less than 5.5%
Triple-pass, double glass and longitudinal fins	*present study*	The highest EXEF was 5.636%
	present study	The highest EXEF was 6.698%

Figure 11 compares the three best cases of the multi-pass SAC with the SPWF type according to the criteria. The TEF, EEF, and EXEF of the DPLF type increase by 2.54–2.68%, 2.44–2.61%, and 0.345–0.417% compared with SPWF type; see Figure 11(a). The TEF, EEF, and EXEF of the TPLF type are about 7.99–8.17%, 7.89–8.08%, and 1.296–1.328% higher than the SPWF type; see Figure 11(b).

Figure 12 compares the EEF and EXEF of the three best cases of the present study with contemporary work; the single-pass SAC with V-down perforated baffles and multi-pass SAC without fins are considered [47,56]. The EEF and EXEF of the TPLF type are better than the DPLF type. The multi-pass SAC with fins is higher EEF and EXEF than the multi-pass SAC without fins. The multi-pass SAC is less the EEF than the V-down SAC, and the EXEF is the opposite. It shows the harmony of exergy performance and efficiency in the present results, and multi-pass SAC with longitudinal fins yielded promising results.

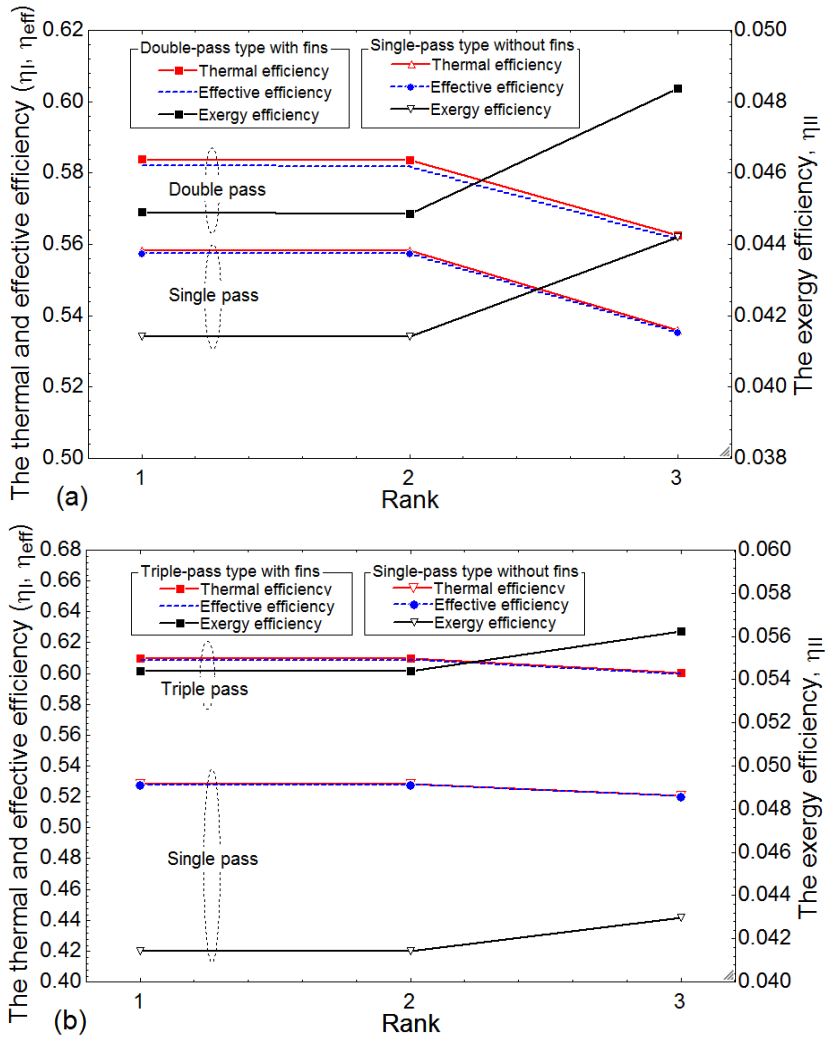

Fig. 11. Compare the efficiency for three best cases (a) the DPLF with SPWF type (b) TPLF with SPWF type

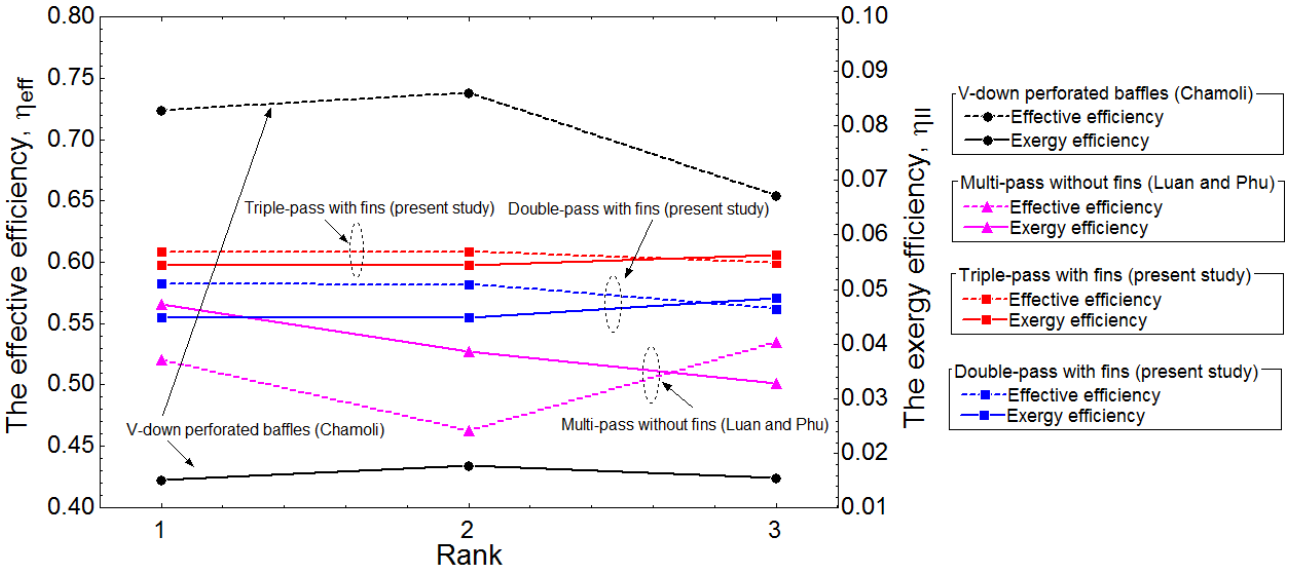

Fig. 12. Compare three best cases of present model, V-down [56], multi-pass without fin [47]

5. Conclusions

This study investigated the exergy efficiency, effective efficiency, and optimization of multi-pass solar air collectors with longitudinal fins. Multi-objective optimization by the PSI method with three maximum criteria: thermal efficiency, effective efficiency, and exergy efficiency. There are 625 cases surveyed for each type, with the range of 0.01–0.02 kg/s air flow rate, 1–3 m collector length, 15–35 mm collector depth, and 24.21–30.67 mm fin pitch. The main findings are as follows

i. The triple-pass SAC with longitudinal fins has better thermal efficiency, effective efficiency, and exergy efficiency than the double-pass SAC with longitudinal fins on average 2.99%, 3.01%, and 0.9% for best cases.
ii. The highest exergy efficiency of triple-pass and double-pass with longitudinal fins was 6.698% and 5.636% at m = 0.01 kg/s, H = 20 mm, L = 3 m, F_p = 30.67 mm.
iii. The highest effective efficiency of triple-pass and double-pass with longitudinal fins was 69.09% and 66.17% at m = 0.02 kg/s, H = 15 mm, L = 1 m, F_p = 24.21 mm.
iv. The thermal efficiency, effective efficiency, and exergy efficiency were 58.38%, 58.22%, and 4.491% for the best case of double-pass SAC with longitudinal fins (m = 0.0175 kg/s, H = 15 mm, L = 2.5 m, F_p = 30.67 mm). They were 2.56%, 2.47%, and 0.35% better than the single-pass SAC without fin.
v. The thermal efficiency, effective efficiency, and exergy efficiency were 60.97%, 60.85%, and 5.439% for the best case of triple-pass SAC with longitudinal fins (m = 0.0125 kg/s, H = 15 mm, L = 2 m, F_p = 25.56 mm). They were 8.17%, 8.08%, and 1.296% better than the single-pass SAC without fin.
vi. The good configuration of double-pass SAC with longitudinal fins at L = 2.5 m, H = 15 mm, F_p = 28.75–30.67 mm, m = 0.15 – 0.175 kg/s. The good configuration of triple-pass at L = 2 m, H = 15 mm, F_p = 24.21–25.56 mm, m = 0.0125kg/s. These are configurations that can be referenced for design.
vii. The worst case for the multi-pass SAC is the configuration with a short collector length, large collector depth, and large fin pitch.

Acknowledgement

This research is supported by Ho Chi Minh City University of Technology and Education (HCMUTE), Vietnam.

References

[1] Said, Zafar, Prabhakar Sharma, L. Syam Sundar, Changhe Li, Duy Cuong Tran, Nguyen Dang Khoa Pham, and Xuan Phuong Nguyen. "Improving the thermal efficiency of a solar flat plate collector using MWCNT-Fe3O4/water hybrid nanofluids and ensemble machine learning." *Case Studies in Thermal Engineering* 40 (2022): 102448. https://doi.org/10.1016/j.csite.2022.102448

[2] Said, Zafar, Prabhakar Sharma, Rajvikram M. Elavarasan, Arun Kumar Tiwari, and Manish K. Rathod. "Exploring the specific heat capacity of water-based hybrid nanofluids for solar energy applications: A comparative evaluation of modern ensemble machine learning techniques." *Journal of Energy Storage* 54 (2022): 105230. https://doi.org/10.1016/j.est.2022.105230

[3] Lang, Kwong Cheng, Lian See Tan, Jully Tan, Azmi Mohd Shariff, and Hairul Nazirah Abdul Halim. "Life cycle assessment of potassium lysinate for biogas upgrading." *Progress in Energy and Environment* 22 (2022): 29-39. https://doi.org/10.37934/progee.22.1.2939

[4] Nguyen, Thanh Luan, An Quoc Hoang, and Duong Hung Hoang. "Study on Predicting the Gasification Process of Acacia Wood on a Downdraft Gasifier: Using the Non-stoichiometric Equilibrium Model." *Journal of Technical Education Science* 72A (2022): 10-18. https://doi.org/10.54644/jte.72A.2022.1119

[5] Al Rizeiqi, Nasser Mohammed, Nasser Al Rizeiqi, and Ali Nabavi. "Potential of Underground Hydrogen Storage in Oman." *Journal of Advanced Research in Applied Sciences and Engineering Technology* 27, no. 1 (2022): 9-31. https://doi.org/10.37934/araset.27.1.931
[6] Rebhi, Redha, Younes Menni, Giulio Lorenzini, and Hijaz Ahmad. "Forced-Convection Heat Transfer in Solar Collectors and Heat Exchangers: A Review." *Journal of Advanced Research in Applied Sciences and Engineering Technology* 26, no. 3 (2022): 1-15. https://doi.org/10.37934/araset.26.3.115
[7] Said, Zafar, Shek Rahman, Prabhakar Sharma, Ahmed Amine Hachicha, and Salah Issa. "Performance characterization of a solar-powered shell and tube heat exchanger utilizing MWCNTs/water-based nanofluids: an experimental, numerical, and artificial intelligence approach." *Applied Thermal Engineering* 212 (2022): 118633. https://doi.org/10.1016/j.applthermaleng.2022.118633
[8] Prasad, B. N., and J. S. Saini. "Effect of artificial roughness on heat transfer and friction factor in a solar air heater." *Solar Energy* 41, no. 6 (1988): 555-560. https://doi.org/10.1016/0038-092X(88)90058-8
[9] Sahu, Mukesh Kumar, and Radha Krishna Prasad. "Thermohydraulic performance analysis of an arc shape wire roughened solar air heater." *Renewable Energy* 108 (2017): 598-614. https://doi.org/10.1016/j.renene.2017.02.075
[10] Momin, Abdul-Malik Ebrahim, J. S. Saini, and S. C. Solanki. "Heat transfer and friction in solar air heater duct with V-shaped rib roughness on absorber plate." *International Journal of Heat and Mass Transfer* 45, no. 16 (2002): 3383-3396. https://doi.org/10.1016/S0017-9310(02)00046-7
[11] Patel, Sumer Singh, and Atul Lanjewar. "Experimental and numerical investigation of solar air heater with novel V-rib geometry." *Journal of Energy Storage* 21 (2019): 750-764. https://doi.org/10.1016/j.est.2019.01.016
[12] Lanjewar, Atul, J. L. Bhagoria, and R. M. Sarviya. "Experimental study of augmented heat transfer and friction in solar air heater with different orientations of W-Rib roughness." *Experimental Thermal and Fluid Science* 35, no. 6 (2011): 986-995. https://doi.org/10.1016/j.expthermflusci.2011.01.019
[13] Thakur, Sushant, and N. S. Thakur. "Impact of multi-staggered rib parameters of the 'W'shaped roughness on the performance of a solar air heater channel." *Energy Sources, Part A: Recovery, Utilization, and Environmental Effects* (2020): 1-20. https://doi.org/10.1080/15567036.2020.1764672
[14] Ranjan, Rajeev, M. K. Paswan, and N. Prasad. "CFD based analysis of a solar air heater having isosceles right triangle rib roughness on the absorber plate." *International Energy Journal* 17, no. 2 (2017). https://doi.org/10.17485/ijst/2016/v9i38/90171
[15] Gawande, Vipin B., A. S. Dhoble, D. B. Zodpe, and Sunil Chamoli. "Experimental and CFD-based thermal performance prediction of solar air heater provided with chamfered square rib as artificial roughness." *Journal of the Brazilian Society of Mechanical Sciences and Engineering* 38 (2016): 643-663. https://doi.org/10.1007/s40430-015-0402-9
[16] Yadav, Anil Singh, and J. L. Bhagoria. "A numerical investigation of square sectioned transverse rib roughened solar air heater." *International Journal of Thermal Sciences* 79 (2014): 111-131. https://doi.org/10.1016/j.ijthermalsci.2014.01.008
[17] Yeh, Ho-Ming, and Chii-Dong Ho. "Effect of external recycle on the performances of flat-plate solar air heaters with internal fins attached." *Renewable Energy* 34, no. 5 (2009): 1340-1347. https://doi.org/10.1016/j.renene.2008.09.005
[18] Chabane, Foued, Noureddine Moummi, and Said Benramache. "Experimental study of heat transfer and thermal performance with longitudinal fins of solar air heater." *Journal of Advanced Research* 5, no. 2 (2014): 183-192. https://doi.org/10.1016/j.jare.2013.03.001
[19] Bezbaruah, Parag Jyoti, Aabir Das, Rajat Subhra Das, and Bikash Kumar Sarkar. "Numerical Investigation on Triangular Fin-Based Solar Air Heater." In *Advances in Energy Research*, Vol. 2: Selected Papers from ICAER 2017, pp. 341-350. Springer Singapore, 2020. https://doi.org/10.1007/978-981-15-2662-6_31
[20] Manjunath, M. S., K. Vasudeva Karanth, and N. Yagnesh Sharma. "Numerical analysis of flat plate solar air heater integrated with an array of pin fins on absorber plate for enhancement in thermal performance." *Journal of Solar Energy Engineering* 141, no. 5 (2019). https://doi.org/10.1115/1.4043517
[21] Priyam, Abhishek, and Prabha Chand. "Experimental investigations on thermal performance of solar air heater with wavy fin absorbers." *Heat and Mass Transfer* 55 (2019): 2651-2666. https://doi.org/10.1007/s00231-019-02605-1
[22] Singh, Satyender, Ankit Singh, and Subhash Chander. "Thermal performance of a fully developed serpentine wavy channel solar air heater." *Journal of Energy Storage* 25 (2019): 100896. https://doi.org/10.1016/j.est.2019.100896
[23] Luan, Nguyen Thanh, and Nguyen Minh Phu. "Thermohydraulic correlations and exergy analysis of a solar air heater duct with inclined baffles." *Case Studies in Thermal Engineering* 21 (2020): 100672. https://doi.org/10.1016/j.csite.2020.100672

[24] Sharma, Sachin, Randip Kumar Das, and Kishor Kulkarni. "Computational and experimental assessment of solar air heater roughened with six different baffles." *Case Studies in Thermal Engineering* 27 (2021): 101350. https://doi.org/10.1016/j.csite.2021.101350
[25] Nayak, R. K., and S. N. Singh. "Effect of geometrical aspects on the performance of jet plate solar air heater." *Solar Energy* 137 (2016): 434-440. https://doi.org/10.1016/j.solener.2016.08.024
[26] Soni, Akhilesh, and S. N. Singh. "Experimental analysis of geometrical parameters on the performance of an inline jet plate solar air heater." *Solar Energy* 148 (2017): 149-156. https://doi.org/10.1016/j.solener.2017.03.081
[27] El-Sebaii, A. A., S. Aboul-Enein, M. R. I. Ramadan, S. M. Shalaby, and B. M. Moharram. "Investigation of thermal performance of-double pass-flat and v-corrugated plate solar air heaters." *Energy* 36, no. 2 (2011): 1076-1086. https://doi.org/10.1016/j.energy.2010.11.042
[28] Gao, Wenfeng, Wenxian Lin, Tao Liu, and Chaofeng Xia. "Analytical and experimental studies on the thermal performance of cross-corrugated and flat-plate solar air heaters." *Applied Energy* 84, no. 4 (2007): 425-441. https://doi.org/10.1016/j.apenergy.2006.02.005
[29] Kareem, M. W., Khairul Habib, Amjad A. Pasha, Kashif Irshad, L. O. Afolabi, and Bidyut Baran Saha. "Experimental study of multi-pass solar air thermal collector system assisted with sensible energy-storing matrix." *Energy* 245 (2022): 123153. https://doi.org/10.1016/j.energy.2022.123153
[30] Krishnananth, S. S., and K. Kalidasa Murugavel. "Experimental study on double pass solar air heater with thermal energy storage." *Journal of King Saud University-Engineering Sciences* 25, no. 2 (2013): 135-140. https://doi.org/10.1016/j.jksues.2012.05.004
[31] Dabra, Vishal, Laxmikant Yadav, and Avadhesh Yadav. "The effect of tilt angle on the performance of evacuated tube solar air collector: experimental analysis." *International Journal of Engineering, Science and Technology* 5, no. 4 (2013): 100-110. https://doi.org/10.4314/ijest.v5i4.9
[32] Zhang, Ji, and Tingting Zhu. "Systematic review of solar air collector technologies: Performance evaluation, structure design and application analysis." *Sustainable Energy Technologies and Assessments* 54 (2022): 102885. https://doi.org/10.1016/j.seta.2022.102885
[33] Jia, Binguang, Fang Liu, and Da Wang. "Experimental study on the performance of spiral solar air heater." *Solar Energy* 182 (2019): 16-21. https://doi.org/10.1016/j.solener.2019.02.033
[34] Ansari, Mohammad, and Majid Bazargan. "Optimization of flat plate solar air heaters with ribbed surfaces." *Applied Thermal Engineering* 136 (2018): 356-363. https://doi.org/10.1016/j.applthermaleng.2018.02.099
[35] Hernández, Alejandro L., José E. Quiñonez, and Fabio H. López. "Transient numerical study of thermo-energetic performance of solar air heating collectors with metallic porous matrix." *Solar Energy* 178 (2019): 181-192. https://doi.org/10.1016/j.solener.2018.12.035
[36] Ramani, B. M., Akhilesh Gupta, and Ravi Kumar. "Performance of a double pass solar air collector." *Solar Energy* 84, no. 11 (2010): 1929-1937. https://doi.org/10.1016/j.solener.2010.07.007
[37] Setyawan, EkoYohanes, Arif Kurniawan, Febi Rahmadianto, Richard A. M. Napitupulu, and Parulian Siagian. "Flat plate type solar collector performance using double thermal insulation." In *IOP Conference Series: Materials Science and Engineering*, vol. 852, no. 1, p. 012044. IOP Publishing, 2020. https://doi.org/10.1088/1757-899X/852/1/012044
[38] Velmurugan, P., and R. Kalaivanan. "Thermal performance studies on multi-pass flat-plate solar air heater with longitudinal fins: An analytical approach." *Arabian Journal for Science and Engineering* 40 (2015): 1141-1150. https://doi.org/10.1007/s13369-015-1573-5
[39] Naphon, Paisarn. "On the performance and entropy generation of the double-pass solar air heater with longitudinal fins." *Renewable Energy* 30, no. 9 (2005): 1345-1357. https://doi.org/10.1016/j.renene.2004.10.014
[40] Fudholi, Ahmad, Kamaruzzaman Sopian, Mohd H. Ruslan, Mohd Y. Othman, and Muhammad Yahya. "Thermal efficiency of double pass solar collector with longitudinal fins absorbers." *American Journal of Applied Sciences* 8, no. 3 (2011): 254. https://doi.org/10.3844/ajassp.2011.254.260
[41] Garg, H. P., Ranjana Jha, C. Choudhury, and Gouri Datta. "Theoretical analysis on a new finned type solar air heater." *Energy* 16, no. 10 (1991): 1231-1238. https://doi.org/10.1016/0360-5442(91)90152-C
[42] Sivakumar, S., K. Siva, and M. Mohanraj. "Experimental thermodynamic analysis of a forced convection solar air heater using absorber plate with pin-fins." *Journal of Thermal Analysis and Calorimetry* 136 (2019): 39-47. https://doi.org/10.1007/s10973-018-07998-5
[43] Hosseini, Seyedeh Sahar, Abas Ramiar, and Ali Akbar Ranjbar. "Numerical investigation of natural convection solar air heater with different fins shape." *Renewable Energy* 117 (2018): 488-500. https://doi.org/10.1016/j.renene.2017.10.052
[44] Manjunath, M. S., K. Vasudeva Karanth, and N. Yagnesh Sharma. "Numerical analysis of the influence of spherical turbulence generators on heat transfer enhancement of flat plate solar air heater." *Energy* 121 (2017): 616-630. https://doi.org/10.1016/j.energy.2017.01.032

[45] Luan, Nguyen Thanh, and Nguyen Minh Ha. "A study to evaluate the effects of geometrical parameters and flow parameters on the exergy efficiency of tube-in-tube helical heat exchanger by CFD simulation." *Journal of Technical Education Science* 63 (2021): 71-82. https://doi.org/10.54644/jte.63.2021.71
[46] Hedayatizadeh, Mahdi, Faramarz Sarhaddi, Ali Safavinejad, Faramarz Ranjbar, and Hossein Chaji. "Exergy loss-based efficiency optimization of a double-pass/glazed v-corrugated plate solar air heater." *Energy* 94 (2016): 799-810. https://doi.org/10.1016/j.energy.2015.11.046
[47] Luan, Nguyen Thanh, and Nguyen Minh Phu. "First and second law evaluation of multipass flat-plate solar air collector and optimization using preference selection index method." *Mathematical Problems in Engineering* 2021 (2021): 1-16. https://doi.org/10.1155/2021/5563882
[48] Farahani, Somayeh Davoodabadi, and Milad Shadi. "Optimization-decision making of roughened solar air heaters with impingement jets based on 3E analysis." *International Communications in Heat and Mass Transfer* 129 (2021): 105742. https://doi.org/10.1016/j.icheatmasstransfer.2021.105742
[49] Akpinar, Ebru Kavak, and Fatih Koçyiğit. "Energy and exergy analysis of a new flat-plate solar air heater having different obstacles on absorber plates." *Applied Energy* 87, no. 11 (2010): 3438-3450. https://doi.org/10.1016/j.apenergy.2010.05.017
[50] Duffie, John A., and William A. Beckman. *Solar engineering of thermal processes*. John Wiley & Sons, 2013. https://doi.org/10.1002/9781118671603
[51] Phu, Nguyen Minh, and Nguyen Thanh Luan. "A review of energy and exergy analyses of a roughened solar air heater." *Journal of Advanced Research in Fluid Mechanics and Thermal Sciences* 77, no. 2 (2021): 160-175. https://doi.org/10.37934/arfmts.77.2.160175
[52] Velmurugan, P., and R. Kalaivanan. "Energy and exergy analysis of solar air heaters with varied geometries." *Arabian Journal for Science and Engineering* 40 (2015): 1173-1186. https://doi.org/10.1007/s13369-015-1612-2
[53] Matheswaran, M. M., T. V. Arjunan, and D. Somasundaram. "Analytical investigation of solar air heater with jet impingement using energy and exergy analysis." *Solar Energy* 161 (2018): 25-37. https://doi.org/10.1016/j.solener.2017.12.036
[54] Kurtbas, Irfan, and Aydın Durmuş. "Efficiency and exergy analysis of a new solar air heater." *Renewable Energy* 29, no. 9 (2004): 1489-1501. https://doi.org/10.1016/j.renene.2004.01.006
[55] Esen, Hikmet. "Experimental energy and exergy analysis of a double-flow solar air heater having different obstacles on absorber plates." *Building and Environment* 43, no. 6 (2008): 1046-1054. https://doi.org/10.1016/j.buildenv.2007.02.016
[56] Chamoli, Sunil. "Preference selection index approach for optimization of V down perforated baffled roughened rectangular channel." *Energy* 93 (2015): 1418-1425. https://doi.org/10.1016/j.energy.2015.09.125
[57] Chauhan, Ranchan, Tej Singh, N. S. Thakur, and Amar Patnaik. "Optimization of parameters in solar thermal collector provided with impinging air jets based upon preference selection index method." *Renewable Energy* 99 (2016): 118-126. https://doi.org/10.1016/j.renene.2016.06.046
[58] Maniya, Kalpesh, and Mangal Guido Bhatt. "A selection of material using a novel type decision-making method: Preference selection index method." *Materials & Design* 31, no. 4 (2010): 1785-1789. https://doi.org/10.1016/j.matdes.2009.11.020
[59] Benhamza, Abderrahmane, Abdelghani Boubekri, Abdelmalek Atia, Hicham El Ferouali, Tarik Hadibi, Müslüm Arıcı, and Naji Abdenouri. "Multi-objective design optimization of solar air heater for food drying based on energy, exergy and improvement potential." *Renewable Energy* 169 (2021): 1190-1209. https://doi.org/10.1016/j.renene.2021.01.086
[60] Klein, Sanford A., and F. Alvarado. "Engineering equation solver software (EES)." F-*Chart Software: Madison*, WI, USA (2013).
[61] Yeh, Ho-Ming, and Tong-Tshien Lin. "The effect of collector aspect ratio on the collector efficiency of flat-plate solar air heaters." *Energy* 20, no. 10 (1995): 1041-1047. https://doi.org/10.1016/0360-5442(95)00053-J
[62] Velmurugan, P., and R. Kalaivanan. "Energy and exergy analysis in double-pass solar air heater." *Sādhanā* 41 (2016): 369-376. https://doi.org/10.1007/s12046-015-0456-5
[63] Assadeg, J., Ali HA Al-Waeli, A. Fudholi, and K. Sopian. "Energetic and exergetic analysis of a new double pass solar air collector with fins and phase change material." *Solar Energy* 226 (2021): 260-271. https://doi.org/10.1016/j.solener.2021.08.056
[64] Bahrehmand, D., M. Ameri, and M. J. R. E. Gholampour. "Energy and exergy analysis of different solar air collector systems with forced convection." *Renewable Energy* 83 (2015): 1119-1130. https://doi.org/10.1016/j.renene.2015.03.009
[65] Abo-Elfadl, Saleh, Mohamed S. Yousef, M. F. El-Dosoky, and Hamdy Hassan. "Energy, exergy, and economic analysis of tubular solar air heater with porous material: an experimental study." *Applied Thermal Engineering* 196 (2021): 117294. https://doi.org/10.1016/j.applthermaleng.2021.117294

[66] Abo-Elfadl, Saleh, Mohamed F. El-Dosoky, and Hamdy Hassan. "Energy and exergy assessment of new designed solar air heater of V-shaped transverse finned absorber at single-and double-pass flow conditions." *Environmental Science and Pollution Research* 28 (2021): 69074-69092. https://doi.org/10.1007/s11356-021-15163-z

[67] Singh, Varun Pratap, Siddharth Jain, Ashish Karn, Ashwani Kumar, Gaurav Dwivedi, Chandan Swaroop Meena, and Raffaello Cozzolino. "Mathematical Modeling of Efficiency Evaluation of Double-Pass Parallel Flow Solar Air Heater." *Sustainability* 14, no. 17 (2022): 10535. https://doi.org/10.3390/su141710535